Input impedance analysis on a capillary pipe with a longitudinal thermal gradient

A. Zaker[a], S. Guilain[b] et V. Gibiat[c]
[a]Institut clément ader, 3 rue caroline aigle, 31400 Toulouse, France
[b]Renault, 1 Allée Cornuel, 91510 Lardy, France
[c]Institut Clément Ader, 3 rue Caroline Aigle, 31400 Toulouse, France
ashkan.zaker@univ-tlse3.fr

Input impedance primarily used in the analysis of musical instruments, has shown to be an asset in the car manufacturing industries to improve the engine intake efficiencies. Air to liquid charge-air coolers used in new internal combustion engines impose a steep longitudinal thermal gradient on the intake air contained in its capillary passages. Therefore, the effect of a tapered rectangular longitudinal thermal gradient and its shape on the input impedance and the reflection function of a semi-infinite capillary pipe and an open-ended capillary pipe was numerically studied. The FE method incorporated utilizes the low reduced frequency model to calculate the acoustic pressure. The thermal gradient creates a distinct impulse response. The results showed that the shape of gradient and its intensity impact the input impedance and that the acoustic response related to the open-end condition is considerably more important than the one caused by the thermal gradient. This study will be accompanied by an experimental analysis in a future paper.

1 Introduction

Air pollution caused by internal combustion engines has been one of the major reasons of global warming and many regulations have been applied to control the emission of pollutants. In 2015, the European legislations forbade the emission of more than 130 gr/km of CO_2 for passenger cars and this threshold will reduce to 95 gr/km by 2021. This obligation along with concerns regarding climate change has led to the development of new technologies.

The improvement of engine's intake efficiency is regarded as one, which is done through multiple technologies such as using dynamic energy in the acoustic waves generated by engine called acoustic pressure tuning.

Hence, an intelligent design of intake system can be beneficial to engine's volumetric efficiency [1]. Conventionally, pressure wave tuning is done through the resonance analysis of intake system. The impact of pressure wave tuning can be up to 30% depending on engine speed.

Nitrogen oxides are another dangerous family of pollutants, one way to reduce which is to control the intake air temperature using intercoolers [2]. This process leads to strong thermal gradients along short distances, specially in water-cooled charge-air coolers (WCAC). Their acoustic analysis, however, has been concentrated on the impact of their geometry on acoustic attenuation [3–5]. In [4], for example, The analysis was done on various geometries with the same thermal gradient and hence not analyzing the possible acoustic impact of thermal discontinuities.

the majority of studies on the interaction of field gradients and acoustic propagation have had their applicability in exhaust system and combustion chambers [6, 7]. However, in the field of musical acoustics, this interaction has been reported to have flattening effect on the sound of musical instruments being played in low temperatures and with longitudinal gradients of as low as 15°K [8, 9].

Peat in his article [10], analyzed the impact of mean flow and a small linear thermal gradient on the acoustic propagation in engine exhaust line.An approximate analytical solution has been also developed by Documacy which is valid for higher frequencies in domains having a background temperature gradient [11, 12]. An exact one dimensional analytical solution has been derived for linear and exponential gradient by Sujith et al. [13], quadratic in [14] and polynomial case in [15].

None of the mentioned studies focuses on a localized thermal gradient. The tapered rectangular thermal gradient at various longitudinal locations on a circular capillary pipe and a semi-infinite boundary condition used in this study, permits to see a clear response both in time and frequency domain whereas in previous studies, the gradient encompassed the entirety of the computation domain.

2 Theoretical and numerical tools

2.1 Low reduced frequency model

The acoustic propagation in pipes with viscous and thermal losses has been the subject of much work [16–18]. Some of the primary and important studies on these cases are done by Kirchhoff and Reynolds. The studies on the acoustic propagation in the air shows that in the absence of walls, the acoustic energy attenuation is very low except for high frequencies. However, these losses in the enclosed passages such as pipe must be considered [19]. Losses are mostly concentrated in the viscous and thermal boundary layers, the thickness of which depends on the medium properties and the frequency.

Many authors have driven various reduced solutions, the principle of many of which being to model the pipes either as wide, narrow or in between. This narrowness is defined based on the reduced frequency, $k = 2r\pi/l$ with l being the wavelength, and the shear wave number, $s = r\sqrt{\rho\omega/\mu}$ where, ρ is air density, ω is the angular velocity, μ is the dynamic viscosity and the low reduced frequency model (LRF) is used here. According to Beltman, this method is more efficient in all cases including the visco-thermal losses than the full linearized Navier Stokes equations (LNS) [20]. Theoretically, the validity of this model is:

$$k << 1, \frac{k}{s} << 1 \quad . \tag{1}$$

In the finite element analysis done, 10 quadratic elements per wave length (for $f = 100kHz$) are used and the maximum frequency is set to be 100kHz leading to a time resolution of 1e-6s. The frequency resolution is 1Hz.

2.2 Air properties

Apart from the thermal gradient, the fields of density and sound speed are temperature-dependent. Besides, conductivity, viscosity, constant-volume specific heat capacity and constant-pressure specific heat capacity are used as functions of temperature and therefore location using empirical relations [21]. However, the background pressure field is assumed uniform.

2.3 Inlet impedance

Being defined as:

$$\bar{Z} = \frac{p}{u\rho c} \quad , \tag{2}$$

normalized acoustic impedance shows the frequency response of a system to an excitation signal which shows the resonances of the system and the amplitude of each resonance at the corresponding frequency. The first use of this parameter was in the musical instrument industry and then in other fields such as car manufacturing industries [22–24]. Temporal analysis in this paper is done using the reflection function which is the inverse Fourier transform of the reflection coefficient defined as:

$$r(t) = \sum_{\omega=-\infty}^{+\infty} \left(\frac{\bar{Z}(\omega) - 1}{\bar{Z}(\omega) + 1}\right) \exp(i\omega t) \quad . \tag{3}$$

In order to reduce the Gibbs effect when doing the inverse Fourier transform, an unsymmetrical tapered window is used to reduce mostly the response in high frequencies.

3 Case-studies and results

The capillary pipe has a diameter of 1.6mm and a length of 1.7m leading to an open-end resonance of 50Hz in case of neglecting losses and a cut-off frequency of 120kHz. The shape of the cross section being of little importance [5], the triangular cross-section passage in the WCAC has been modeled by a circular cross section one.

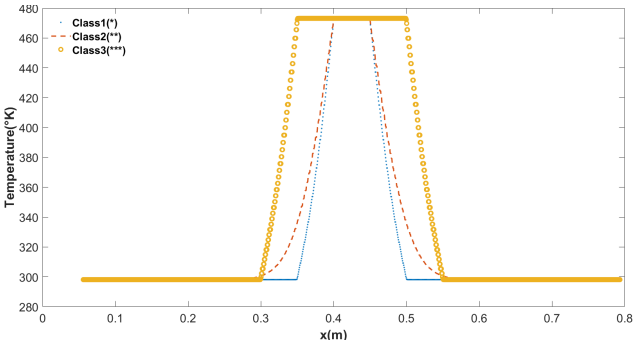

Figure 1: Three classes of longitudinal thermal gradient profile

The axial temperature decrease of air in a WCAC being more than 150°C over about 5 cm led to the selection of a thermal gradient reaching from 473°K to 298°K along the same length in the cases studied.

- Class 1(*)

Adiabatic and heated section length is 5cm.

- Class 2(**)

Length of adiabatic segment is 15cm and the heated section 5cm.

- Class 3(***)

Length of adiabatic segment is 5cm and the heated section 10cm.

The adiabatic boundary condition segments are at the two sides of the heated segment (Figure 2). $X(m)$ being the location of the end of the heated segment, cases with the semi-infinite boundary condition are as in the Table 1 where the class of the gradient used for each case is written in parenthesis with a star sign (*).

Table 1: Thermal boundary conditions

	Case(*)	Case(**)	Case(***)	X(m)
1		1-1	1-1-1	0.45
2		-	-	0.9
3		-	-	1.35

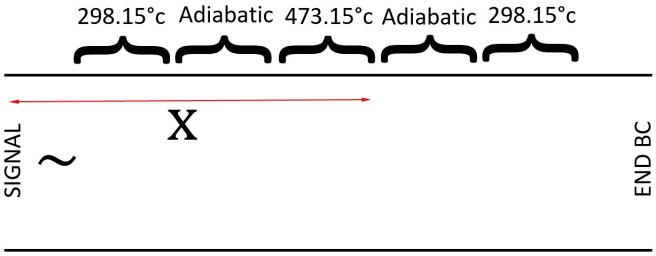

Figure 2: Thermal boundary conditions

Using a highly localized thermal gradient with such low diameter, the normalized characteristic acoustic impedance of the medium is only slightly modified and hence, its frequency domain analysis is done more conveniently. The Cases with open-end boundary condition have an additional "O" at the end of their names (Ex. case1O). Finally, Cases without field discontinuities are called Case0 and Case0O.

3.1 Frequency domain

The thermal gradient acts similarly to a geometry discontinuity, leading to a distinct frequency and time domain response. Hence, the type of thermal gradient used here must lead to two distinct responses mixed together. This fact is implied in the complexity of the frequency response in Figure 3. The difference in the amplitude of the frequency domain response shows the attenuation due to viscosity. As the gradient gets farther from the excitation signal, the amplitude of its response is damped more and its first resonance frequency reduces as in Figure 3.

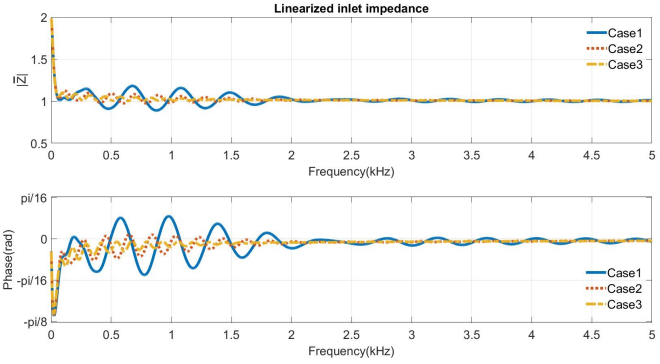

Figure 3: The effect of gradient location on the inlet impedance of a semi-infinite capillary pipe

Besides, the response depends on the gradient slope. Higher slope leads to more acoustic reflection as in figure below where, the amplitude of the majority of resonance frequencies reduces with reducing slope (Figure 4).

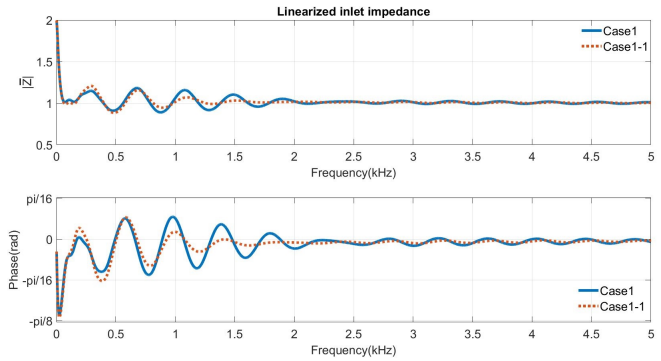

Figure 4: The effect of gradient slope on the inlet impedance of a semi-infinite capillary pipe

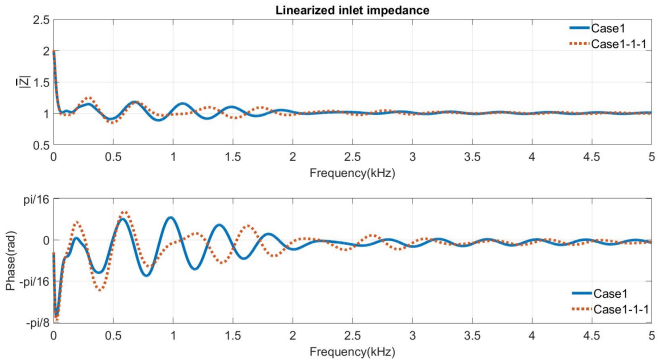

Figure 5: The effect of length of the heated section on the inlet impedance of a semi-infinite capillary pipe

The length of the high temperature section has a different impact on lower and higher frequencies. As this length increases, the resonance amplitude increases in low frequencies and reduces in higher frequencies (Figure 5).

3.2 Time domain

In the time domain, the reflection function reveals domain discontinuities. Increase and decrease of temperature produces two distinct impulse responses at the location of gradient. Two pics of reflection function are distanced by about 10cm. To locate the pics of the function correctly, an accurate sound speed is required in the region with the thermal gradient. Using the the average temperature, the first minimum is found in around $x = 0.4m$ and the maximum around $x = 0.5m$ (Figure 6).

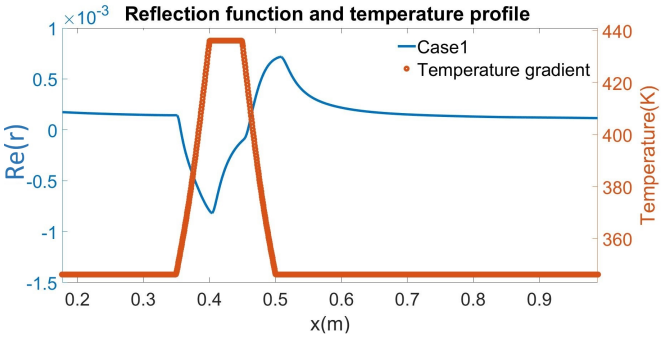

Figure 6: Case 1 and corresponding thermal gradient profile

The response of case 3O shows that the open-end reflection is considerably more important than that caused by the thermal gradient (Figure 7a). This case compared with Case1 shows the role of high visco-thermal losses, where the thermal gradient response is higher than the one caused by open-end which shows how important is the location of thermal gradient in such highly attenuative pipes. Moreover, a comparison of class1 and class 2 of gradients show the modified shape of impulse and reducing its steep pic which is due to the modified shape of gradient in class 2. Besides, the intensity of impulse reduces. The class 3 does not produce a considerable effect apart from being closer to signal location and being a bit less attenuated. In the capillary pipe studied here, the pics of the reflection function are much attenuated due to thermo-viscous losses (Figure 7b).

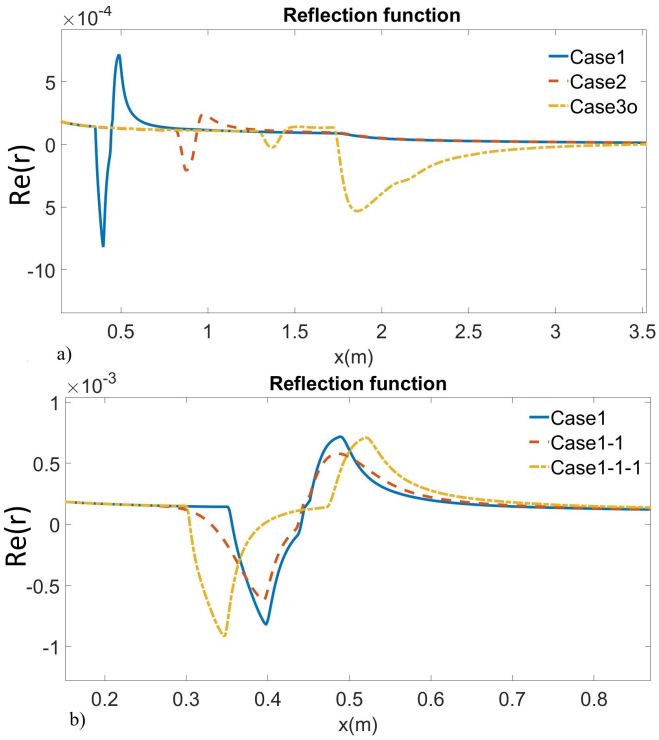

Figure 7: Reflection function. a) Effect of distance of a discontinuity in specific acoustic impedance, b) Effect of the shape of the gradient

4 Conclusion

The effect of the presence of a sharp longitudinal thermal gradient in a long capillary pipe was analyzed using a purely numerical approach. The length of the gradient being small compared to the total length of the pipe, has made it possible to reduce the effect of general change in propagation velocity and hence to facilitate the analysis of thermal gradient effect in frequency domain. The results showed how the thermal gradient can be important in a very special case of highly attenuating capillary pipe compared to an open-end reflection, located much farther from the source than the thermal gradient. The same analysis taking into account various diameters could be helpful to conclusively evaluate the effect of thermal gradient.

References

[1] D. Broom, Induction RAM, *Automobile Engineer*, 130 (1969).

[2] United States Environmental Protection Agency, Nitrogen Oxides (NOx), Why and How They Are Controlled, (1999). Available on https://www3.epa.gov/ttncatc1/dir1/fnoxdoc.pdf

[3] M. Knutsson, M. Abom, Acoustic analysis of charge air coolers, *SAE International*, (2007).

[4] H. Mezher, J. Migaud, Optimized Air Intake for a Turbocharged Engine Taking into Account Water-Cooled Charge Air Cooler Reflective Properties for Acoustic Tuning, *SAE International*, (2013).

[5] M. Knutsson, M. Abom, Acoustic modelling of Charge Air Coolers, *J. Vib. Acoust.* ***139***, (2017).

[6] K. S. Peat, R. Kirby, Acoustic wave motion along a narrow cylindrical duct in the presence of an axial mean flow and temperature gradient, *J. Acoust. Soc. Am.* ***107***, 1859 (1999).

[7] M. Hoeijmakers, V. Kornilova, I. Lopez Arteagaab, P. de Goey, H. Nijmeijer, Flame dominated thermoacoustic instabilities in a system with high acoustic losses, *J. Combust. Flame.* ***169***, 209 (2016).

[8] N. H. Fletcher, T. D. Rossing, *The Physics of Musical Instruments*, Springer, New York (1991).

[9] M. Vollmer, K. P. Mollmann, *Infrared Thermal Imaging: Fundamentals, Research and Applications*, Springer, New York (2011).

[10] K. S. Peat, The transfer matrix of a uniform duct with a linear temperature gradient, *J. Sound Vib.* ***123***, 43 (1988).

[11] E. Documaci, Transmission of sound in uniform pipes carrying hot gas flows, *J. Sound Vib.* ***195***, 257 (1996).

[12] E. Documaci, An approximate annalytical solution for plane sound wave transmission in inhomogeneous ducts, *J. Sound Vib.* ***217***, 853 (1998).

[13] R. I. Sujith, G. A. W. Sujith, B. T. Zinn, An exact solution for one-dimensional acoustic fields in ducts with an axial temperature gradient, *J. Sound Vib.* ***184***, 389 (1995).

[14] B. Manoj Kumar, R. I. Sujith, Exact solution for one-dimensional acoustic fields in ducts with a quadratic mean temperature profile, *J. Acoust. Soc. Am.* ***101***, 3798 1997).

[15] B. Manoj Kumar, R. I. Sujith, Exact solution for one-dimensional acoustic fields in ducts with polynomial mean temperature profile, *J. Sound Vib.* ***120***, 965 (1998).

[16] G. Kirchhoff, Ueber den Einfluss der Wärmeleitung in einem Gase auf die Schallbewegung, *Annalen der physik* ***210***, 177 (1863).

[17] J. W. Strutt, B. Rayleigh, *The Theory of Sound*, The Macmillan Company, London (1877).

[18] H. V. Helmholtz, Verhandlungen der Naturhistorisch-Medizinischen Vereins zu Heidelberg, (1863).

[19] P. M. Morse, K. U. Ingard, *Theoretical acoustics*, Princton University Press, Princton (1986).

[20] W. M. Beltman, Viscothermal wave propagation including acousto-elastic interaction, part 1: Theory, *J. Sound Vib.* ***227***, 555 (1999).

[21] J. C. Dixon, *The Shock Absorber Handbook*, John Wiley and sons, West Sussex (2007).

[22] V. Gibiat, F, Laloë, Acoustical impedance measurements by the two microphone- three-calibration (TMTC) method, *J. Acoust. Soc. Am.* ***88***, 2533 (1990).

[23] P. Dickens, J. Smith, Improved precision in measurements of acoustic impedance spectra using resonance-free calibration loads and controlled error distribution, *J. Acoust. Soc. Am.* ***121***, 1471 (2007).

[24] J. Backus, Input impedance curves for the reed woodwind instruments, *J. Acoust. Soc. Am.* ***56***, 1266 (1974).